

Original citation:

Andersson, Robert, Jirstrand, Mats, Peletier, Lambertus, Chappell, M. J. (Michael J.), Evans, Neil D. and Gabrielsson, Johan. (2016) Dose–response-time modelling : second-generation turnover model with integral feedback control. European Journal of Pharmaceutical Sciences, 81 . pp. 189-200.

Permanent WRAP URL:

<http://wrap.warwick.ac.uk/97880>

Copyright and reuse:

The Warwick Research Archive Portal (WRAP) makes this work by researchers of the University of Warwick available open access under the following conditions. Copyright © and all moral rights to the version of the paper presented here belong to the individual author(s) and/or other copyright owners. To the extent reasonable and practicable the material made available in WRAP has been checked for eligibility before being made available.

Copies of full items can be used for personal research or study, educational, or not-for-profit purposes without prior permission or charge. Provided that the authors, title and full bibliographic details are credited, a hyperlink and/or URL is given for the original metadata page and the content is not changed in any way.

Publisher's statement:

© 2015. This manuscript version is made available under the CC-BY-NC-ND 4.0 license
<http://creativecommons.org/licenses/by-nc-nd/4.0/>

A note on versions:

The version presented here may differ from the published version or, version of record, if you wish to cite this item you are advised to consult the publisher's version. Please see the 'permanent WRAP URL' above for details on accessing the published version and note that access may require a subscription.

For more information, please contact the WRAP Team at: wrap@warwick.ac.uk

Dose-response-time modelling: Second-generation turnover model with integral feedback control

Robert Andersson^{a,*}, Mats Jirstrand^b, Lambertus Peletier^c, Michael J. Chappell^a, Neil D. Evans^a, Johan Gabrielsson^d

^a*School of Engineering, University of Warwick, Coventry, United Kingdom*

^b*Fraunhofer-Chalmers Centre, Chalmers Science Park, Göteborg, Sweden*

^c*Mathematical Institute, Leiden University, Leiden, The Netherlands*

^d*Division of Pharmacology and Toxicology, Department of Biomedical Sciences and Veterinary Public Health, Swedish University of Agriculture Sciences, Uppsala, Sweden*

Abstract

This study presents a dose-response-time (DRT) analysis based on a large pre-clinical biomarker dataset on the interaction between nicotinic acid (NiAc) and free fatty acids (FFA). Data were collected from studies that examined different rates, routes, and modes of NiAc provocations on the FFA time course. All information regarding the exposure to NiAc was excluded in order to demonstrate the utility of a DRT model. Special emphasis was placed on the selection process of the biophase model. An inhibitory I_{\max} -model, driven by the biophase amount, acted on the turnover rate of FFA. A second generation NiAc/FFA model, which encompasses integral (slow buildup of tolerance - an extension of the previously used NiAc/FFA turnover models) and moderator (rapid and oscillatory) feedback control, was simultaneously fitted to all time courses in normal rats. The integral feedback control managed to capture an observed 90% adaptation (i.e., almost a full return to baseline) when 10 days constant-rate infusion protocols of NiAc were used. The half-life of the adaptation process had a 90% prediction interval between 3.5-12 h in the present population. The pharmacodynamic parameter estimates were highly consistent when compared to an exposure-driven analysis, partly validating the DRT modelling approach and suggesting the potential of DRT analysis in areas where exposure data are not attainable. Finally, new numerical algorithms, which rely on sensitivity equations to robustly and efficiently compute the gradients in the parameter optimization, were successfully used for the mixed-effects approach in the parameter estimation.

Keywords: Biophase models, Turnover, Tolerance, Feedback control, Nicotinic acid (NiAc), Free fatty acids (FFA)

*Corresponding author

Email address: r.k.andersson@warwick.ac.uk (Robert Andersson)

1. Introduction

The traditional pharmacokinetic-pharmacodynamic (PK-PD) modelling approach is generally based on known plasma kinetics when the PD properties are assessed. Dose-response-time (DRT) data analysis is an alternative to exposure-driven kinetic - dynamic modelling when exposure data are sparse or lacking. This involves studies where the pharmacological response precedes the systemic exposure (e.g. pulmonary drug administration) or when the drug is locally administered (e.g. in ophthalmics). In DRT analyses the pharmacological effect is assumed to contain some kinetic properties whereby a biophase function can be developed and in turn acts as a ‘driving’ function of the pharmacological effect. The biophase function is assessed using various structures from a biophase model library when the DRT model is fitted to data. This biophase library consists of feasible models derived from the kinetic information in the response-time course in combination with knowledge of the physiology.

DRT data analysis dates back to the 1960’s and 1970’s when Smolen [53, 54, 55] and Levy [39] introduced the concept. Smolen used response data to quantify the bioavailability and biokinetic behaviour of a mydriatic drug after oral and ophthalmic administration whilst Levy derived a relation between the pharmacological effect and elimination rate of a mydriatic drug. Since the work of Smolen, DRT data analysis has been proven to be applicable to novel systems where the kinetics and/or dynamics behave non-linearly, when there are time-delays in the response data, and when the system contains feedback mechanisms [24]. The technique has successfully been applied in models of the muscle relaxant drug vecuronium [14, 22, 21, 64], antinociceptive drugs [1, 26, 24], ophthalmic drugs [24, 41], antidepressants [28], psycho-motor stimulants [26], drugs to treat chronic obstructive pulmonary disease (COPD) [65], and osteoporosis [46]. For a review and theoretical guide to DRT analysis see Gabrielsson et al. [24, 26]. DRT models go under the name of K-PD (K for kinetic) models in some analyses [28, 29, 35, 46, 65]. However, in the latter case the biophase turnover rate, rather than the biophase amount, is driving the response.

NiAc has long been used as a therapeutic agent to treat dyslipidemia. The drug effectively suppresses the level of triglycerides and low-density lipoprotein cholesterol in plasma whilst elevating the level of high-density lipoprotein cholesterol [16]. NiAc inhibits hydrolysis in adipose tissue by activating the G-coupled receptor GPR109A, which in turn inhibits the adenylyl cyclase, leading to reduced levels of cyclic adenosine monophosphate (cAMP). The cAMP activates the enzyme protein kinase A which phosphorylates hormone-sensitive lipase that in turn hydrolyses triglycerides into FFA (Fig. 1) [44].

We sought to further demonstrate the utility of DRT data analysis. To do so, we analysed a rich preclinical data set containing several individuals (a total of 95 rats and response-time courses) and provocations (constant rate infusions at three dosage levels, step-wise increasing infusion at two dosage levels, and oral administration at three dosage levels) of the NiAc - FFA interaction. Available exposure data for NiAc were intentionally excluded in order to use a DRT approach. The developed DRT model was compared and validated by means of

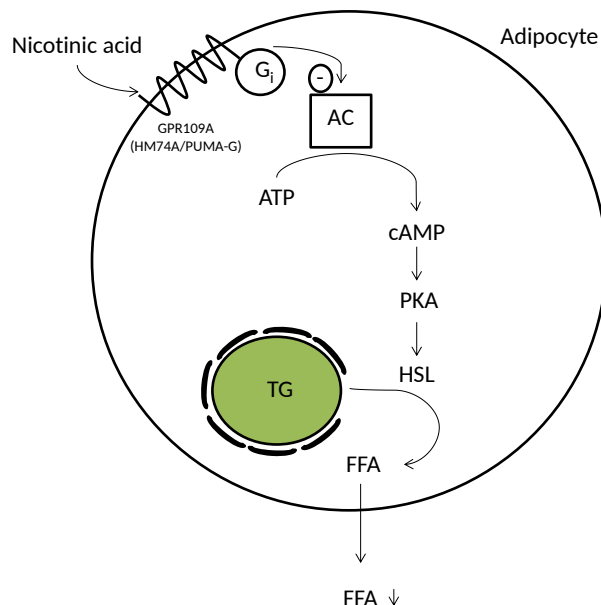


Figure 1: Mechanism of NiAc-induced inhibition of lipolysis. NiAc activates the G-coupled receptor GPR109A, which in turn inhibits the adenylyl cyclase, reducing the production of cyclic adenosine monophosphate (cAMP) from adenosine triphosphate. cAMP activates protein kinase A, which phosphorylates hormone-sensitive lipase, thereby regulating the hydrolysis of triglycerides into FFA. Thus, NiAc binding will inhibit lipolysis leading to reduced levels of FFA. Adapted from Offermanns 2006 [44].

exposure-driven kinetic/dynamic results, where the pharmacokinetic properties of NiAc had been thoroughly characterized [3].

The applied pharmacodynamic model is an extended and significantly improved version of a previously utilised feedback model [2, 4, 6, 25, 59]. This second-generation feedback model uses an integral feedback control mechanism to capture the slowly developing tolerance. This model is affected by a biophase model that drives the inhibitory drug-mechanism function. The biophase model was selected using an iterative modelling approach where the biophase model was systemically refined in order to better capture the dynamic behaviour seen in the data. This study presents an approach to the development of the biophase model structure simultaneously with the pharmacodynamic model. In light of the aforementioned, DRT analyses do not fully replace exposure-driven analyses, particularly in safety assessment.

2. Materials and methods

2.1. Background and data sources

The pre-clinical data set consisted of FFA response-time series of 95 male Sprague-Dawley rats under NiAc provocation. These data have previously been described by Ahlström et al. [3, 5, 7, 4, 6, 33] and Tapani et al. [59]. A thorough description of the animals and surgical procedure, experimental design, and analytical assay can be found in Ahlström et al. [4].

All experiments were designed and conducted at AstraZeneca, Mölndal Sweden, and approved by the Ethics Committee for Animal Experiments, Gothenburg, Sweden (EA 100868).

2.2. Selection process of biophase models

The DRT data analysis is based on the assumption that the pharmacological response contains some kind of kinetic information and is driven by NiAc in a hypothetical biophase compartment. The fit of the pharmacodynamic model (given in Sec. 2.4) to the data informs about the soundness of choice of the driving biophase function. Depending on the route of administration, the input is either approximated to be directly into the biophase (intravenous dosing) or absorbed into the biophase (oral dosing). The biophase model structures were modified through a series of steps where data from different routes and rates of administration were sequentially assessed (see Table 1). In a pairwise accept-reject procedure, two models were qualitatively and quantitatively compared and the one considered to be the better model, in terms of goodness-of-fit, was selected and further challenged by more complex data (see Table 1). The goodness-of-fit was based on the likelihood function value and by graphical inspection of the function plots.

Step I. The first biophase model that was evaluated consisted of a zero-order input into and first-order elimination from the biophase (Fig. 2b). To capture the disposition characteristics, the model was evaluated using response-time data derived from different constant-rate intravenous infusion experiments.

Step II. The next biophase model to be evaluated consisted of zero-order input and Michaelis-Menten elimination from the biophase (Fig 2c). This model was evaluated using the same data as in step I.

The model that best described (in terms of goodness-of-fit) the dynamics, using the response-time data derived from different constant-rate intravenous infusion experiments, was kept for the later stages of the biophase evolution. In this case, the models used in step I and II had close to similar objective function values and were indistinguishable by graphical inspection of the function fits. However, in accordance with the principle of Occam's razor, and by applying the *Akaike Information Criterion* [8], the zero-order input and first-order elimination model was chosen.

100 *Step III.* When a model for the biophase elimination model was set, response-time data derived from experiments for different oral dosages were included in order to address the biophase absorption. The first biophase absorption model that was evaluated consisted of first-order input and elimination from the biophase (Fig. 2d).

105 *Step IV.* The final absorption model that was evaluated consisted of Michaelis-Menten input and first-order elimination (Fig 2e). This model was evaluated using the same data as in step III.

The model in step IV had a higher likelihood function value and a substantially better fit when inspecting the function plots than the model in step III, and was therefore selected.

110 2.3. The final biophase model

The biophase was modelled as

$$\frac{dA_b}{dt} = Inf - k \cdot A_b, \quad (1)$$

for intravenous administration of NiAc, with initial condition

$$A_b(0) = 0 \quad (2)$$

115 where A_b denotes the biophase drug amount, k the biophase elimination rate constant, and Inf the infusion rate to the biophase. The infusion rate was modelled as a step function with either constant rate during the infusion period, or stepwise decreasing infusion rates, to mimic the infusion regimens used in the experiments.

Orally administered NiAc was assumed to be eliminated from the gut according to a Michaelis-Menten type of saturable process

$$\frac{dA_g}{dt} = -\frac{V_{\max,g} \cdot A_g}{K_{m,g} + A_g} \quad (3)$$

120 with initial condition

$$A_g(0) = D \quad (4)$$

125 where A_g denotes the amount of drug in the gut, $V_{\max,g}$ the maximal elimination rate from the gut, $K_{m,g}$ the Michaelis-Menten constant (representing the amount in the gut at half maximal rate), and D the oral drug dose. The drug amount that is eliminated from the gastro-intestinal tract is absorbed into the biophase, giving the biophase equation

$$\frac{dA_b}{dt} = \frac{V_{\max,g} \cdot A_g}{K_{m,g} + A_g} - k \cdot A_b \quad (5)$$

with initial condition

$$A_b(0) = 0 \quad (6)$$

where A_b denotes the biophase drug amount and k the biophase elimination rate constant.

2.4. Structure of the FFA feedback model

130 The fundamental dynamics of FFA are described in terms of a turnover equation

$$\frac{dR}{dt} = \tilde{k}_{in} - \tilde{k}_{out} \cdot R \quad (7)$$

where R denotes the FFA level, and \tilde{k}_{in} and \tilde{k}_{out} are functions describing the lumped effects of NiAc, and insulin and other hormones, on the turnover and fractional turnover of FFA, respectively. The NiAc-induced action on FFA is
135 described by means of an inhibitory drug mechanism function given by

$$I(A_b) = 1 - \frac{I_{max} \cdot A_b^\gamma}{ID_{50}^\gamma + A_b^\gamma} \quad (8)$$

where A_b denotes the biophase drug amount, I_{max} the efficacy, ID_{50} the potency, and γ the Hill exponent.

The FFA level in the model is affected by a chain of moderator compartments M_1, \dots, M_8 . These moderator compartments represent a conglomerate
140 of insulin, and other hormonal, regulators of the FFA disposition. Insulin, for example, acts as a dual regulator on the FFA level via rapid inhibition of the lipolysis and slow re-esterification of FFA to triglycerides [23, 50, 58]. This is captured by the dynamics of the first M_1 and the last M_8 moderator compartment, respectively. The moderators are described by the following set of
145 equations

$$\begin{aligned} \frac{dM_1}{dt} &= k_{tol} \cdot (R - M_1) \\ \frac{dM_2}{dt} &= k_{tol} \cdot (M_1 - M_2) \\ &\vdots \\ \frac{dM_8}{dt} &= k_{tol} \cdot (M_7 - M_8) \end{aligned} \quad (9)$$

where R denotes the FFA level and k_{tol} the fractional turnover rate of the moderators. Consequently, all moderator compartments have the same transit time of $1/k_{tol}$. The moderators are initially assumed to be in equilibrium with the response, thus

$$M_1(0) = \dots = M_8(0) = R_0 \quad (10)$$

150 where R_0 is the FFA baseline level. The number of moderator compartments selected was previously discussed by Ahlström et al. [7].

Long-term exposure to NiAc has proven to induce insulin resistance in adipocytes [20, 47]. This is believed to be a consequence of down-regulated gene expressions

of the insulin and β -adrenergic pathways in adipose tissue [32]. Insulin resistance ultimately leads to full systemic adaptation with a FFA level that returns to its baseline within a few days [37, 45]. This slow and complete adaptation is captured by an integral feedback controller, with output $u(t)$, that slowly forces deviating FFA levels back towards their baseline R_0 despite persistent perturbations such as constant rate infusion of NiAc. The integral controller is given by

$$u(t) = K_i \int_0^t \left(1 - \frac{R(\tau)}{R_0}\right) d\tau \quad (11)$$

where K_i denotes the integral gain parameter (here-after referred to as the adaptation rate). The integral controller may also be expressed as a rate equation

$$\frac{du}{dt} = K_i \cdot \left(1 - \frac{R(t)}{R_0}\right) \quad (12)$$

with initial condition

$$u(0) = 0. \quad (13)$$

The expanded turnover equation of FFA under NiAc provocation is given by

$$\begin{aligned} \frac{dR}{dt} = & k_{\text{in}} \cdot (1 + u(t)) \cdot \frac{1}{\left(\frac{M_1}{R_0}\right)^p} \cdot I(A_b) \\ & - k_{\text{out}} \cdot \left(\frac{M_8}{R_0}\right) \cdot R \end{aligned} \quad (14)$$

with initial condition

$$R(0) = R_0 \quad (15)$$

where R denotes the FFA level, k_{in} the basal turnover rate, k_{out} the basal fractional turnover rate, R_0 the baseline of response, $u(t)$ the integral controller, p the amplification factor, and M_1 and M_8 the first and last moderator, respectively. The moderators are normalized in the turnover Eq. 14 with the baseline FFA value R_0 . The levels of the moderators follow the level of the FFA according to Eq. 9. In turn, the first moderator M_1 modifies the turnover rate k_{in} , amplified with the exponent p , whilst the last moderator M_8 modifies the fractional turnover rate k_{out} . These feedback mechanisms represent the fast inhibition of lipolysis and the slower re-esterification of FFA to triglycerides, triggered by insulin and other hormones, that strive to dampen fluctuations in the FFA level. Furthermore, when the FFA level drops below the baseline level, the integral controller, given by Eq. 11, will accumulate and provide a positive contribution to the turnover rate k_{in} of FFA. Similarly, when the FFA level increases and rises above the baseline level, the integral controller will accumulate and provide a negative contribution to the turnover rate. The full pharmacodynamic model structure is depicted in Fig 3.

2.5. Initial parameter estimates

At time zero, before administration of NiAc, the system is in steady-state, with the moderators set at R_0 . Consequently, the turnover equation (Eq. 14) pre-NiAc administration is given by

$$\frac{dR}{dt} = k_{\text{in}} - k_{\text{out}} \cdot R_0 = 0. \quad (16)$$

A simple rearrangement gives the relation

$$R_0 = \frac{k_{\text{in}}}{k_{\text{out}}} \quad (17)$$

and hence the system may be simplified with one of the parameters R_0 , k_{in} , or k_{out} removed in the parameter estimation. In this study, k_{in} was estimated as a secondary parameter from the product of R_0 and k_{out} . The initial estimate of the FFA baseline level R_0 was taken as the mean response at time zero.

Since the minimum FFA level is close to zero, initially for high NiAc dosages, we conclude that NiAc has a high efficacy and that I_{max} is close to 1. Furthermore, for high NiAc infusion rates, the inhibitory drug-mechanism function becomes saturated whilst the moderators are initially in steady-state with the response. Using this, and the initiate estimate of I_{max} Eq. 14 can be approximated as

$$\frac{dR}{dt} \approx -k_{\text{out}} \cdot R \quad (18)$$

or

$$R(t) \cong R_0 e^{-k_{\text{out}} t}. \quad (19)$$

By means of this relation, k_{out} can be estimated from the initial down-swing of the response on a semi-logarithmic scale.

The Hill exponent γ and the amplification factor p were initially set to 1 since little was known about the respective parameter values. The remaining parameters were estimated from simulations of the system.

2.6. Modelling random effects and residual variability

The extent of the data set allowed for mixed-effects to be included in the model, i.e., specific parameter values were allowed to vary within the population. To identify which parameters had a significant spread in the population, individual parameter fitting was applied. The five parameters with highest variability, in terms of coefficient of variation, were then selected as individual parameters; the rest were considered as population parameters. The parameters chosen to vary in the population were k , K_i , R_0 , k_{out} , and k_{tol} . These parameters were assumed to be uncorrelated (to simplify the model) and log-normally distributed (to keep the parameters positive).

The individual parameter estimates are referred to as Empirical Bayes Estimates (EBE's) and their individual fits and the model assumptions were quantified by their corresponding η -shrinkage [51, 13].

2.7. Parameter estimation

The parameter estimation of the DRT model in this study was performed using a mixed-effects modelling framework implemented in Mathematica, developed at the Fraunhofer-Chalmers Research Centre for Industrial Mathematics (Gothenburg, Sweden) [9]. This framework is designed to estimate parameters in non-linear mixed effects models where the underlying dynamical system is either described by a set of ordinary or stochastic differential equations. The framework relies on the first-order conditional estimation (FOCE) [38], with or without interactions, to estimate the individual likelihoods of the population likelihood function. The argument that maximises the population likelihood function is found using the Broyden–Fletcher–Goldfarb–Shanno algorithm [43] where the gradient of the objective function is calculated using the so-called *sensitivity equations*.

3. Results

Observed response-time series with corresponding population model fits and 90% Monte Carlo prediction intervals [49] are illustrated in Fig. 4. The FFA concentrations were suppressed in all animals receiving NiAc. A clear adaptation towards the FFA baseline was only seen for the individuals that received a 300 min constant rate infusion of NiAc (Fig. 4d-4f). This functional adaptation was more pronounced the higher the infusion rate. All infusion regimens gave rise to a rebound effect, i.e., the FFA level overshoots the initial baseline, after the infusions were stopped. The rebound effect was more pronounced the higher the infusion rate. This effect was followed by apparent oscillations in the FFA level around the baseline, which were more pronounced with the extended NiAc infusion regimens (longer duration of the infusions and higher NiAc doses). The rats that received an oral dose of NiAc experienced an FFA drop followed by an approximately constant FFA level (Fig. 4i-4k). The higher the dose, the longer the rats stayed at a suppressed and approximately constant FFA level. This was followed by rebound and oscillations. The suppression of FFA, the occurrence of rebound, and the extent of the oscillations were more pronounced the higher the oral dose.

The estimated population biophase amount-time courses are illustrated in Fig. 5. For the constant rate NiAc infusions, the biophase amount quickly reached steady-state (Fig. 5a-5f). The wash-out kinetics were rapid with a half-life of around 2 min. For the highest oral doses, the biophase amount declined in a non-linear fashion post-peak due to absorption-rate limited elimination of NiAc (Fig. 5k).

Observed individual FFA response-time series with individually fitted FFA response levels are illustrated in Fig. 6 for one individual per administration route and rate. The model captured the individual behaviour for all individuals. Specifically, the slow adaptation, in the individuals that received a 300-min infusion of NiAc, was captured by the integral feedback control present in the pharmacodynamic model (Fig. 6d-6f).

260 The fitted population parameters and inter-individual variations with corresponding relative standard errors for the full system are illustrated in Table 2. The biophase elimination rate constant k and the fractional turnover rate of FFA k_{out} are of the same order of magnitude, indicating little to no time-delay between biophase kinetics and FFA dynamics. Since the absorption into the
 265 biophase is non-linear, we observed typical absorption-rate limited elimination at higher oral doses of NiAc. The estimated $K_{\text{m,g}}$ of about $40 \mu\text{mol kg}^{-1}$ implies that the two higher oral doses (81.2 and $812 \mu\text{mol kg}^{-1}$) approach and exceed saturation.

The efficacy parameter I_{max} was estimated as $0.893 < 1$; therefore, NiAc
 270 cannot completely suppress FFA levels. The estimated biophase potency ID_{50} shows that the drug-mechanism function (Eq. 8) will be saturated at the highest infusions and for all the oral doses (Fig. 5). The estimated Hill exponent γ indicates a steep NiAc biophase amount - FFA response relationship at equilibrium. The rate constants k_{out} , k_{tol} , and K_i all have different orders of magnitude, and
 275 thus act over different time-scales. Half-lives for the three rate constants with 90% non-parametric bootstrap prediction intervals [18] are given in Table 3.

The pivotal systems (k_{out} , k_{tol} , K_i , p) and drug parameters (I_{max} , γ) were compared to estimates from an exposure-driven analysis, using the same dynamic model. The estimates are given in Table 4.

280 3.1. Model predictions

By using the predicted population parameters, we explored the long-term effects of NiAc provocation on FFA level for the infusion rate of $0.17 \mu\text{mol kg}^{-1} \text{min}^{-1}$ (Fig. 7), aiming at a therapeutic plasma concentration of NiAc of $1 \mu\text{mol}$ [4]. The model predicted 90% adaptation within approximately 10 days of constant
 285 NiAc exposure. The effect of the fast moderator (M_1) feedback can be seen immediately after the initial drop, where the system rapidly returns towards the baseline. The effect of the slower moderator feedback (M_8) is seen as a slower terminal return with oscillations in the FFA level. The effect of the integral feedback controller is seen as the slow return to baseline over time.

290 3.2. Structural identifiability

The model structure was proven to be structurally locally identifiable. Identifiability was tested using the Exact Arithmetic Rank (EAR) approach [11, 36, 48]. This approach requires that the functions in the system of differential equations are rational polynomial expressions in the variables and parameters.
 295 In this study, the inhibitory drug-mechanism function and the feedback function of the first moderator compartment did not fulfil this requirement since the state variables were raised to the powers of γ and p , respectively (which are real-valued). However, this problem is solved by re-writing the system in rational form by the introduction of auxiliary variables [40]. For example, let

$$B(t) = A_b^\gamma(t) \quad (20)$$

$$B(0) = B_0 (= A_b^\gamma(0)). \quad (21)$$

300 Then we have that

$$\frac{dB}{dt} = \gamma \frac{B(t)}{A_b(t)} \cdot \frac{dA_b}{dt}, \quad (22)$$

and by introducing the parameter $\widetilde{ID}_{50}(=ID_{50}')$ the non-rational functions in the inhibitory drug-mechanism function can be written as

$$1 - \frac{I_{\max} \cdot B(t)}{\widetilde{ID}_{50} + B(t)} \quad (23)$$

which is a rational expression of the parameters and the variables.

3.3. Shrinkage analysis

305 Shrinkage analysis was used in order to quantify the individual parameter assumptions (log-normality) and to quantify the model fits [51]. The η -shrinkage of the EBE's are given in Table 2. The standard deviation of the residual additive error and the ε -shrinkage for the infusion and oral data are given in Table 5.

310 4. Discussion

DRT data analysis has previously proved to be an alternative approach to exposure-driven modelling when exposure data are sparse or absent [14, 22, 21, 24, 26, 35, 41, 64, 65]. The technique has been applied in studies of novel systems where the pharmacodynamic response behaves non-linearly, where time-lags are present, and when functional adaptation is manifested [24]. These examples demonstrate the potential of DRT modelling in characterizing mechanisms of action of complex pharmacological systems. The present study extends the utility of a non-linear biophase model, permitting the description of more complex absorption kinetics. The non-invasiveness of DRT analysis promotes its use when excessive sampling is prohibited (small animals, paediatric populations) [60].

4.1. DRT modelling

DRT data analysis typically requires response-time series with higher resolution than traditional traditional exposure-driven studies. This is because kinetic information in response-time data are sought for the biophase turnover.

325 In contrast to exposure-driven pharmacodynamic modelling, the biophase kinetics and the pharmacodynamic properties of a DRT model must be estimated simultaneously. This may in some instances lead to difficulties in separating confounding factors originating from either the concentration-time or the response-time course or both. If, for example, drug absorption and disposition is highly non-linear this may confound the interpretation of nonlinear pharmacodynamics. Therefore, *a priori* knowledge about the mechanism(s) of action is necessary for construction of an adequate biophase model.

4.2. Strategy when selecting the biophase model

335 The structure of the biophase model is preferably derived through a series of steps where data from different administration routes are sequentially implemented and the biophase is structure refined if necessary. In this way, different properties, for example elimination rate and absorption rate, can be addressed separately.

340 In this study, the intravenous data were initially analysed in order to address the biophase disposition. Both a linear first-order and a Michaelis-Menten elimination model were successfully fitted to the data. The two models had approximately the same objective function values and fitted the data equally well when the function plots were inspected graphically. However, when the AIC
345 was applied, the simpler model was preferred, and therefore selected. The similarity between the linear first-order and Michaelis-Menten elimination models was due to the high estimate of the Michaelis-Menten constant, in comparison to the biophase amounts, rendering an approximately linear elimination rate at all dose levels.

350 When the disposition model was set, oral data were included and the absorption process into the biophase was assessed. Both a first-order and nonlinear Michaelis-Menten absorption model were fitted to the data. The first-order absorption model failed to capture the full dynamic behaviour of the data in that it systematically over-predicted the response-time course for the highest
355 oral dose ($81.2 \mu\text{mol kg}^{-1}$). This problem was resolved by the Michaelis-Menten absorption model that also captured the absorption-rate limited elimination.

4.3. The NiAc/FFA DRT model

The model captures the general trends of the populations and the Monte Carlo prediction intervals span most of the individuals.

360 The population fits in Fig. 4 indicate that the population medians differ slightly from the individual behaviours for the infusion of $0.033 \mu\text{mol kg}^{-1} \text{min}^{-1}$ (Fig. 4a), which is predicted to be higher than the individual outcomes, and the oral dose of $81.2 \mu\text{mol kg}^{-1}$ (Fig. 4i), which is predicted to be lower than the individual outcomes. This difference is believed to be an artefact of inter-
365 occasional variability since these populations have lower (for the infusion of $0.033 \mu\text{mol kg}^{-1} \text{min}^{-1}$), respectively higher (for the oral dose of $81.2 \mu\text{mol kg}^{-1}$), baseline values than the estimated population baseline. A potential way to avoid this issue is to model the inter-occasional variations.

370 The eight moderator compartments were chosen to model the slow and fast action of insulin and other hormones. A more eloquent way would be to optimize the number of compartments as a system parameter or use another time-delay relation, such as the actual insulin concentration-time course. This is a matter for future model refinement.

375 The integral feedback control, moderator feedback, and the turnover of FFA are shown to act over different time-scales (Table 3). Turnover of FFA occurs within minutes, the feedback triggered by insulin and other hormones operates within 30 minutes, while the slow buildup of NiAc tolerance occurs within a

couple of hours.

380 The model predicts full system adaptation for long-term constant rate infusions with the therapeutic infusion rate of $0.17 \mu\text{mol kg}^{-1} \text{min}^{-1}$ (Fig. 7). This illustrates the effect of the integral feedback control, which forces the response back to baseline over time. Homeostatic behaviour has been proven experimentally in studies of long-term NiAc provocation [45]. However, 90% of adaptation typically occurs within 24 h at therapeutic concentrations of NiAc. A better estimate for the adaptation K_i is expected when longitudinal data are generated
385 and added to the analysis.

In general, there is high consistency between our derived system parameter estimates and the ones from exposure-driven analysis. The slight deviations are still within reasonable biological limits given the parameter uncertainty (Table
390 4). This comparison strengthens the use of DRT analysis as a complementary technique in studies where limited exposure data are available.

The proposed biophase model is *per se* a substantial simplification in comparison to the original multi-compartment plasma kinetics (exposure) model that has been applied by others (Iwaki et al. [34], Ahlström et al. [7] and
395 Tapani et al. [59]). Therefore, dose predictions, impact of different dosing regimens, or assessment of safety margins will probably require an exposure-driven approach.

This study has demonstrated the utility of DRT modelling by developing biophase-driven pharmacodynamic models. The biophase structure was challenged by means of different rates, routes, and modes of administration, on top
400 of the pharmacodynamic complexities.

We envision that DRT data analysis will have great significance on pharmacological responses (biomarkers) used in the future assessment of dynamics. DRT analysis has proven to be an acceptable alternative to exposure-driven PD
405 modelling in situations where plasma concentrations are sparse or missing, or if extreme differences are seen for the initial and terminal disposition phases in plasma (such as with oligonucleotides, where rate and extent of exposure vary significantly between tissues [15, 31]).

4.4. Control theory

410 In this study, techniques from systems and control theory were utilized to describe feedback mechanisms and systemic adaptation. By applying integral feedback control the system demonstrated full adaptation under constant long-term NiAc pressure (see Fig. 7). In fact, integral feedback control is a prerequisite for perfect adaptation in systems that experience constant disturbance
415 [10, 56].

The control theory feature of the pharmacodynamic model provides a significant improvement in comparison to previously published NiAc/FFA models [7, 59], and will make the model better suited for chronic regimens.

Many biological systems, experiencing adaptation when put under external
420 disturbance, have been successfully modelled by means of control theory techniques, including metabolic networks [30], synthetic biology [17], the osmoregulation in yeast [27, 42], and bacterial chemotaxis [12, 66]. El-Samad et al.

showed how integral feedback control could, for example, be derived from enzymatic relations when the goal is to address the control of plasma calcium levels [19]. Control theory techniques have been used sparsely within PK-PD modelling and mostly in dose control [52, 57, 61, 63, 62]. Control theory techniques have a clear potential in modelling intrinsic control and feedback systems.

4.5. Inter-individual and intra-individual variability

When the model was fitted for each individual separately (i.e., without a mixed-effects approach) the parameter estimates of R_0 , k , k_{out} , k_{tol} , and K_i had large coefficients of variation, indicating that the data contained enough information to estimate the corresponding η 's of these parameters (i.e. the individual parameters) in a mixed-effects approach. However, no parametric model (e.g., normal or log-normal) was successfully matched to the distributions of the EBE's. Regardless, a log-normal distribution was chosen to model the EBE's spread due the positive range of the log-normal distribution, a generic feature expected in the parameters. Use of a log-normal model led to high levels of shrinkage in some of the EBE's. Whilst R_0 and k had low η -shrinkages, indicating that the log-normal assumption on the parameter distributions was reasonable, the remaining three parameters (k_{out} , k_{tol} , and K_i) had high η -shrinkages of 40 – 60%, indicating that the log-normal distribution does not describe these parameters in a satisfactory way. Thus, one should be careful not to over-interpret the values of the EBE's. This includes EBE vs EBE plots or EBE vs covariate plots, which are not reliable under high levels of shrinkage. For that reason, analyses of these kinds are omitted in this study. However, the estimated random effects are still useful when describing the data and when extrapolating to, for example, other dosing regimens.

Both of the models used for the infusion and oral data gave reasonably low ε -shrinkages of less than 10% indicating that the models describe the data in a satisfactory manner without being over-fitted.

4.6. New numerical algorithms

The new numerical algorithms used rely on sensitivity equations to calculate the gradients in the optimization routine. This improves precision and accuracy extensively in comparison to finite difference approximations, increasing the chance of convergence in the parameter estimation for computer-intensive models [9].

5. Conclusions

A DRT model was successfully fitted to all time courses available of the NiAc-induced changes in FFA in normal rats, showing the versatility of this approach. A nonlinear biophase model was used to describe saturable absorption. Using moderator compartments, and systems and control theory, we captured different feedback mechanisms. The systems and control theory techniques was successfully applied to describe complete system adaptation under constant long-term

exposure to NiAc. This provides a significant improvement of the previously
465 used NiAc/FFA models and will be suited in chronic regimens. Consistency in
pharmacodynamic parameters between biophase- and kinetic-driven studies in-
dicates potentially wider use of DRT data analysis. New numerical approaches
were successfully applied to robustly and efficiently compute the gradients in
the nonlinear mixed-effects framework.

470 DRT analysis is generally a poorly explored area that has great potential
and could be considered more frequently in future pharmacological studies when
drug exposure data are scarce or even lacking.

Acknowledgements

This work was funded through the Marie Curie FP7 People ITN European
475 Industrial Doctorate (EID) project, IMPACT (Innovative Modelling for Phar-
macological Advances through Collaborative Training) (No. 316736)

Joachim Almquist at Fraunhofer-Chalmers Centre is greatly acknowledged
for valuable scientific discussions and technical assistance.

Appendix A

480 The following is an excerpt from the modelling code used, implemented in
Mathematica. An executable version of this code, with corresponding data sets
used for this study, is available from the authors upon request.

References

- [1] Abou Hammoud, H., Simon, N., Urien, S., Riou, B., Lechat, P., Aubrun, F.,
485 Jul. 2009. Intravenous morphine titration in immediate postoperative pain
management: population kinetic-pharmacodynamic and logistic regression
analysis. *Pain* 144 (1-2), 139–46.
URL <http://www.ncbi.nlm.nih.gov/pubmed/19435651>
- [2] Ackerman, E., Rosevear, J. W., McGuckin, W. F., 1964. A Mathematical
490 Model of the Glucose-tolerance test. *Phys. Med. Biol.* 9, 203–213.
- [3] Ahlström, C., 2011. Modelling of tolerance and rebound in normal and
diseased rats. Dissertation, University of Gothenburg.
- [4] Ahlström, C., Kroon, T., Peletier, L. A., Gabrielsson, J., Dec. 2013. Feed-
back modeling of non-esterified fatty acids in obese Zucker rats after nico-
495 tinic acid infusions. *J. Pharmacokinet. Phar.* 40 (6), 623–38.
URL <http://www.ncbi.nlm.nih.gov/pubmed/24114415>
- [5] Ahlström, C., Peletier, L. A., Gabrielsson, J., Oct. 2011. Quantitative anal-
ysis of rate and extent of tolerance of biomarkers: application to nicotinic
acid-induced changes in non-esterified fatty acids in rats. *Eur. J. Pharm.*
500 *Sci.* 44 (3), 250–64.
URL <http://www.ncbi.nlm.nih.gov/pubmed/21856416>

- [6] Ahlström, C., Peletier, L. A., Gabrielsson, J., Aug. 2013. Challenges of a mechanistic feedback model describing nicotinic acid-induced changes in non-esterified fatty acids in rats. *J. Pharmacokinet. Phar.* 40 (4), 497–512.
- 505 [7] Ahlström, C., Peletier, L. A., Jansson-Löfmark, R., Gabrielsson, J., Feb. 2011. Feedback modeling of non-esterified fatty acids in rats after nicotinic acid infusions. *J. Pharmacokinet. Phar.* 38 (1), 1–24.
URL <http://www.pubmedcentral.nih.gov/articlerender.fcgi?artid=3020290&tool=pmcentrez&rendertype=abstract>
- 510 [8] Akaike, H., 1974. A New Look at the Statistical Model Identification. *IEEE T. Automat. Contr.* 19 (6), 716–723.
- [9] Almquist, J., Leander, J., Jirstrand, M., Mar. 2015. Using sensitivity equations for computing gradients of the FOCE and FOCEI approximations to the population likelihood. *J. Pharmacokinet. Phar.* 42 (3), 191–209.
515 URL <http://link.springer.com/10.1007/s10928-015-9409-1>
- [10] Ang, J., Bagh, S., Ingalls, B. P., Mcmillen, D. R., 2010. Considerations for using integral feedback control to construct a perfectly adapting synthetic gene network. *J Theor Biol* 266 (4), 723–738.
URL <http://dx.doi.org/10.1016/j.jtbi.2010.07.034>
- 520 [11] Anguelova, M., Karlsson, J., Jirstrand, M., Sep. 2012. Minimal output sets for identifiability. *Math. Biosci.* 239 (1), 139–53.
URL <http://www.ncbi.nlm.nih.gov/pubmed/22609467>
- [12] Barkai, N., Leibler, S., 1997. Robustness in simple biochemical networks. *Nature* 387, 913–917.
525 URL http://www.nature.com/nature/journal/v387/n6636/box/387913a0_B0X1.html
- [13] Bonate, P. L., 2011. *Pharmacokinetic-Pharmacodynamic Modeling and Simulation*. Springer, New York.
- 530 [14] Bragg, P., Fisher, D. M., Shi, J., Donati, F., Meistelman, C., Lau, M., Sheiner, L. B., 1994. Comparison of twitch depression of the adductor pollicis and the respiratory muscles. *Pharmacodynamic modeling without plasma concentrations*. *Anesthesiology* 80 (2), 310–319.
- [15] Callies, S., André, V., Patel, B., Waters, D., Francis, P., Burgess, M., Lahn, M., Mar. 2011. Integrated analysis of preclinical data to support the design of the first in man study of LY2181308, a second generation antisense oligonucleotide. *Brit. J. Clin. Pharmacol.* 71 (3), 416–28.
535 URL <http://www.pubmedcentral.nih.gov/articlerender.fcgi?artid=3045551&tool=pmcentrez&rendertype=abstract>
- [16] Carlson, L. A., Aug. 2005. Nicotinic acid: the broad-spectrum lipid drug. A 50th anniversary review. *J. Intern. Med.* 258 (2), 94–114.
540 URL <http://www.ncbi.nlm.nih.gov/pubmed/16018787>

- [17] Cosentino, C., Bates, D., 2011. Feedback Control in Systems Biology. Taylor & Francis Group, Boca Raton.
- 545 [18] Davison, A., Hinkley, D., 1997. Bootstrap Methods and their Application. Cambridge University Press, New York.
- [19] El-Samad, H., Goff, J. P., Khammash, M., Jan. 2002. Calcium homeostasis and parturient hypocalcemia: an integral feedback perspective. J. Theor. Biol. 214 (1), 17–29.
URL <http://www.ncbi.nlm.nih.gov/pubmed/11786029>
- 550 [20] Fabbrini, E., Mohammed, B. S., Korenblat, K. M., Magkos, F., McCrea, J., Patterson, B. W., Klein, S., Jun. 2010. Effect of fenofibrate and niacin on intrahepatic triglyceride content, very low-density lipoprotein kinetics, and insulin action in obese subjects with nonalcoholic fatty liver disease. J. Clin. Endocr. Metab. 95 (6), 2727–35.
555 URL <http://www.pubmedcentral.nih.gov/articlerender.fcgi?artid=2902076&tool=pmcentrez&rendertype=abstract>
- [21] Fisher, D. M., Szenohradszky, J., Wright, P. M. C., 1997. Pharmacodynamic modeling of vecuronium-induced twitch depression. Rapid plasma-effect site equilibration explains faster onset at resistant laryngeal
560 muscles than at the adductor pollicis. Anesthesiology 86 (3), 558–566.
URL http://journals.lww.com/anesthesiology/Abstract/1997/03000/Pharmacodynamic_Modeling_of_Vecuronium_induced.7.aspx
- [22] Fisher, D. M., Wright, P. M. C., 1997. Are plasma concentration values necessary for pharmacodynamic modeling of muscle relaxants? Anesthesiology
565 86 (3), 567–575.
- [23] Frayn, K., Shadid, S., Hamrani, R., Humphreys, S., Clark, M., Fielding, B., Boland, O., Coppsack, S., 1994. Regulation of fatty acid movement in human adipose tissue in the postabsorptive-to-postprandial transition. Am. J. Physiol. Endocrinol. Metab. 266, 308–317.
570 URL <http://ajpendo.physiology.org/content/ajpendo/266/3/E308.full.pdf>
- [24] Gabrielsson, J., Jusko, W., Alari, L., 2000. Modeling of dose–response–time data: four examples of estimating the turnover parameters and generating kinetic functions from response profiles. Biopharm. Drug Dispos. 21 (2),
575 41–52.
URL [http://onlinelibrary.wiley.com/doi/10.1002/1099-081X\(200003\)21:2%3C41::AID-BDD217%3E3.0.CO;2-D/abstract](http://onlinelibrary.wiley.com/doi/10.1002/1099-081X(200003)21:2%3C41::AID-BDD217%3E3.0.CO;2-D/abstract)
- [25] Gabrielsson, J., Peletier, L. A., Oct. 2007. A nonlinear feedback model capturing different patterns of tolerance and rebound. Eur. J. Pharm. Sci. 32 (2), 85–104.
580 URL <http://www.ncbi.nlm.nih.gov/pubmed/17689227>

- [26] Gabrielsson, J., Peletier, L. A., Aug. 2014. Dose-response-time data analysis involving nonlinear dynamics, feedback and delay. *Eur. J .Pharm. Sci.* 59, 36–48.
 585 URL <http://www.ncbi.nlm.nih.gov/pubmed/24751673>
- [27] Gennemark, P., Nordlander, B., Hohmann, S., Wedelin, D., Jan. 2006. A simple mathematical model of adaptation to high osmolarity in yeast. *In Silico Biol* 6 (3), 193–214.
 URL <http://www.ncbi.nlm.nih.gov/pubmed/16922683>
- 590 [28] Gruwez, B., Poirier, M.-F., Dauphin, A., Oli , J.-P., Tod, M., May 2007. A kinetic-pharmacodynamic model for clinical trial simulation of antidepressant action: application to clomipramine-lithium interaction. *Contemp. Clin. Trials* 28 (3), 276–87.
 URL <http://www.ncbi.nlm.nih.gov/pubmed/17059901>
- 595 [29] Hamberg, A.-K., Wadelius, M., Lindh, J. D., Dahl, M. L., Padrini, R., Deloukas, P., Rane, A., Jonsson, E. N., Jun. 2010. A pharmacometric model describing the relationship between warfarin dose and INR response with respect to variations in CYP2C9, VKORC1, and age. *Clin. Pharmacol. Ther.* 87 (6), 727–34.
 600 URL <http://www.ncbi.nlm.nih.gov/pubmed/20410877>
- [30] He, F., Fromion, V., Westerhoff, H. V., 2013. (Im) Perfect robustness and adaptation of metabolic networks subject to metabolic and gene-expression regulation: marrying control engineering with metabolic control. *BMC Syst. Biol.* 7 (131).
 605 URL <http://www.biomedcentral.com/1752-0509/7/131/>
- [31] Heemskerk, H., de Winter, C., van Kuik, P., Heuvelmans, N., Sabatelli, P., Rimessi, P., Braghetta, P., van Ommen, G.-J. B., de Kimpe, S., Ferlini, A., Aartsma-Rus, A., van Deutekom, J. C. T., Jun. 2010. Preclinical PK and PD studies on 2'-O-methyl-phosphorothioate RNA antisense
 610 oligonucleotides in the mdx mouse model. *Mol. Ther.* 18 (6), 1210–7.
 URL <http://www.pubmedcentral.nih.gov/articlerender.fcgi?artid=2889733&tool=pmcentrez&rendertype=abstract>
- [32] Heemskerk, M. M., van den Berg, S. A. A., Pronk, A. C. M., van Klinken, J.-B., Boon, M. R., Havekes, L. M., Rensen, P. C. N., van Dijk, K. W.,
 615 van Harmelen, V., Apr. 2014. Long-term niacin treatment induces insulin resistance and adrenergic responsiveness in adipocytes by adaptive down-regulation of phosphodiesterase 3B. *Am. J. Physiol. Endocrinol. Metab.* 306 (7), E808–13.
 URL <http://www.ncbi.nlm.nih.gov/pubmed/24473440>
- 620 [33] Isaksson, C., Gabrielsson, J., Wallenius, K., Peletier, L. A., Toreson, H., Jan. 2009. Turnover modeling of non-esterified fatty acids in rats after multiple intravenous infusions of nicotinic acid. *Dose-Response* 7 (3),

- 247–69.
 URL <http://www.pubmedcentral.nih.gov/articlerender.fcgi?artid=2754538&tool=pmcentrez&rendertype=abstract>
- [34] Iwaki, M., Ogiso, T., Hayashi, H., Tanino, T., Benet, L. Z., 1996. Acute Dose-Dependent Disposition Studies of Nicotinic Acid in Rats. *Drug Metab. Dispos.* 24 (7), 773–779.
- [35] Jacqmin, P., Snoeck, E., van Schaick, E. A., Gieschke, R., Pillai, P., Steimer, J.-L., Girard, P., Feb. 2007. Modelling response time profiles in the absence of drug concentrations: definition and performance evaluation of the K-PD model. *J. Pharmacokinet. Phar.* 34 (1), 57–85.
 URL <http://www.ncbi.nlm.nih.gov/pubmed/17051439>
- [36] Karlsson, J., Anguelova, M., Jirstrand, M., 2012. An Efficient Method for Structural Identifiability Analysis of Large Dynamic Systems. 16th IFAC Symposium on System Identification (SYSID 2012) 16 (1), 941–946.
- [37] Kroon, T., Kjellstedt, A., Thalén, P., Gabrielsson, J., Oakes, N. D., Sep. 2015. Dosing profile profoundly influences nicotinic acid’s ability to improve metabolic control in rats. *J. Lipid Res.* 56 (9), 1679–1690.
- [38] Leander, J., Lundh, T., Jirstrand, M., 2014. Mathematical Biosciences Stochastic differential equations as a tool to regularize the parameter estimation problem for continuous time dynamical systems given discrete time measurements. *Math Biosci* 251, 54–62.
- [39] Levy, G., 1964. Relationship Between Elimination Rate of Drugs and Rate of Decline of Their Pharmacologic Effects. *J. Pharm. Sci.* 53 (3), 342–343.
- [40] Lindskog, P., 1996. Methods, Algorithms and Tools for System Identification Based on Prior Knowledge. Dissertation, Linköping University.
- [41] Luu, K., Zhang, E., Prasanna, G., 2009. Pharmacokinetic-pharmacodynamic and response sensitization modeling of the intraocular pressure-lowering effect of the EP4 Agonist 5-{3-[(2S)-2-{(3R)-3-hydroxy-4-[3-(trifluoromethyl)phenyl]butyl}-5-oxopyrrolidin-1-yl]propyl}thiophene-2-carboxylate. *J. Pharmacol. Exp. Ther.* 331 (2), 627–635.
 URL <http://jpet.aspetjournals.org/content/331/2/627.short>
- [42] Muzzey, D., Gómez-Urbe, C., Mettetal, J. T., van Oudenaarden, A., 2009. A systems-level analysis of perfect adaptation in yeast osmoregulation. *Cell* 138 (1), 160–171.
 URL <http://www.sciencedirect.com/science/article/pii/S009286740900508X>
- [43] Nocedal, J., Wright, S., 2006. Numerical Optimization. Springer, New York.

- 660 [44] Offermanns, S., Jul. 2006. The nicotinic acid receptor GPR109A (HM74A or PUMA-G) as a new therapeutic target. *Trends Pharmacol. Sci.* 27 (7), 384–90.
URL <http://www.ncbi.nlm.nih.gov/pubmed/16766048>
- [45] Oh, Y., Oh, K., Choi, Y., 2011. Continuous 24-h nicotinic acid infusion
665 in rats causes FFA rebound and insulin resistance by altering gene expression and basal lipolysis in adipose tissue. *Am J Physiol Endocrinol Metab* 300 (2), 1012–1021.
URL <http://ajpendo.physiology.org/content/300/6/E1012.short>
- [46] Pillai, G., Gieschke, R., Goggin, T., Jacqmin, P., Schimmer, R. C., Steimer, J.-L., Dec. 2004. A semimechanistic and mechanistic population PK-PD
670 model for biomarker response to ibandronate, a new bisphosphonate for the treatment of osteoporosis. *Brit. J. Clin. Pharmacol.* 58 (6), 618–31.
URL <http://www.pubmedcentral.nih.gov/articlerender.fcgi?artid=1884644&tool=pmcentrez&rendertype=abstract>
- [47] Poynten, A. M., Gan, S. K., Kriketos, A. D., O’Sullivan, A., Kelly, J. J.,
675 Ellis, B. A., Crisholm, D. J., Campbell, L. V., 2003. Nicotinic acid-induced insulin resistance is related to increased circulating fatty acids and fat oxidation but not muscle lipid content. *Metabolism* 52 (6), 699–704.
- [48] Raue, A., Karlsson, J., Saccomani, M. P., Jirstrand, M., Timmer, J., May
680 2014. Comparison of approaches for parameter identifiability analysis of biological systems. *Bioinformatics* 30 (10), 1440–8.
URL <http://www.ncbi.nlm.nih.gov/pubmed/24463185>
- [49] Robert, C., Casella, G., 2004. Monte Carlo Statistical Methods. Springer, New York.
- [50] Sadur, C., Eckel, R., 1982. Insulin stimulation of adipose tissue lipoprotein
685 lipase. Use of the euglycemic clamp technique. *J. Clin. Invest.* 69 (May), 1119–1125.
URL <http://www.ncbi.nlm.nih.gov/pmc/articles/PMC370176/>
- [51] Savic, R. M., Karlsson, M. O., Sep. 2009. Importance of shrinkage in
690 empirical bayes estimates for diagnostics: problems and solutions. *AAPS J.* 11 (3), 558–69.
URL <http://www.pubmedcentral.nih.gov/articlerender.fcgi?artid=2758126&tool=pmcentrez&rendertype=abstract>
- [52] Schwildren, H., Schüttler, J., Stoeckel, H., 1987. Closed-loop Feedback Control of Methohexital Anesthesia by Quantitative EEF Analysis in Humans.
695 *Anesthesiology* 67, 341–347.
- [53] Smolen, V., Weigand, W., 1973. Drug bioavailability and pharmacokinetic analysis from pharmacological data. *J. Pharmacokinet. Biop.* 1 (4), 329–336.
700 URL <http://link.springer.com/article/10.1007/BF01060040>

- [54] Smolen, V. F., Mar. 1971. Quantitative determination of drug bioavailability and biokinetic behavior from pharmacological data for ophthalmic and oral administrations of a mydriatic drug. *J. Pharm. Sci.* 60 (3), 354–65.
URL <http://www.ncbi.nlm.nih.gov/pubmed/5572111>
- 705 [55] Smolen, V. F., Aug. 1976. Theoretical and computational basis for drug bioavailability determinations using pharmacological data. II. Drug input in equilibrium to response relationships. *J. Pharmacokinet. Biop.* 4 (4), 355–75.
URL <http://www.ncbi.nlm.nih.gov/pubmed/978397>
- 710 [56] Sontag, E. D., Oct. 2003. Adaptation and regulation with signal detection implies internal model. *Syst Control Lett* 50 (2), 119–126.
URL <http://linkinghub.elsevier.com/retrieve/pii/S0167691103001361>
- 715 [57] Stone, A. G. H., Howell, P. R., 2002. Use of the common gas outlet for the administration of supplemental oxygen during Caesarean section under regional anaesthesia. *Anaesthesia* 57, 690–709.
- [58] Strålfors, P., Björgell, P., Belfrage, P., 1984. Hormonal regulation of hormone-sensitive lipase in intact adipocytes: identification of phosphorylated sites and effects on the phosphorylation by lipolytic hormones. *P. Natl. Acad. Sci. USA* 81 (June), 3317–3321.
720 URL <http://www.pnas.org/content/81/11/3317.short>
- [59] Tapani, S., Almquist, J., Leander, J., Ahlström, C., Peletier, L. A., Jirstrand, M., Gabrielsson, J., Aug. 2014. Joint feedback analysis modeling of nonesterified fatty acids in obese Zucker rats and normal Sprague-Dawley
725 rats after different routes of administration of nicotinic acid. *J. Pharm. Sci.* 103 (8), 2571–84.
URL <http://www.ncbi.nlm.nih.gov/pubmed/24986056>
- [60] Tod, M., Dec. 2008. Evaluation of drugs in pediatrics using K-PD models: perspectives. *Fundam. Clin. Pharm.* 22 (6), 589–94.
730 URL <http://www.ncbi.nlm.nih.gov/pubmed/19049659>
- [61] Urquhart, J., Li, C., 1969. Dynamic testing and modeling of adrenocortical secretory function. *Ann. N Y Acad. Sci.*
URL <http://onlinelibrary.wiley.com/doi/10.1111/j.1749-6632.1969.tb14012.x/full>
- 735 [62] Veng-Pedersen, P., Modi, N. B., 1993. A system approach to pharmacodynamics. Input-effect control system analysis of central nervous system effect of alfentanil. *J Pharm Sci* 82 (3), 266–72.
- [63] Vožch, S., Steimer, J.-L., 1985. Feedback Control Methods for Drug Dosage Optimisation. *Clin. Pharmacokinet.* 10 (6), 457–476.

- 740 [64] Warwick, N., Graham, G., Torda, T., 1998. Pharmacokinetic analysis of
the effect of vecuronium in surgical patients: pharmacokinetic and phar-
macodynamic modeling without plasma concentrations. *Anesthesiology*
88 (4), 874–884.
URL [http://journals.lww.com/anesthesiology/Abstract/1998/](http://journals.lww.com/anesthesiology/Abstract/1998/04000/Pharmacokinetic_Analysis_of_the_Effect_of.5.aspx)
745 [04000/Pharmacokinetic_Analysis_of_the_Effect_of.5.aspx](http://journals.lww.com/anesthesiology/Abstract/1998/04000/Pharmacokinetic_Analysis_of_the_Effect_of.5.aspx)
- [65] Wu, K., Looby, M., Pillai, G., Pinault, G., Drollman, A. F., Pascoe, S.,
Feb. 2011. Population pharmacodynamic model of the longitudinal FEV1
response to an inhaled long-acting anti-muscarinic in COPD patients. *J.*
Pharmacokinet. Phar. 38 (1), 105–19.
750 URL <http://www.ncbi.nlm.nih.gov/pubmed/21104005>
- [66] Yi, T. M., Huang, Y., Simon, M. I., Doyle, J., Apr. 2000. Robust perfect
adaptation in bacterial chemotaxis through integral feedback control. *P.*
Natl. Acad. Sci. USA 97 (9), 4649–53.
URL [http://www.pubmedcentral.nih.gov/articlerender.fcgi?](http://www.pubmedcentral.nih.gov/articlerender.fcgi?artid=18287&tool=pmcentrez&rendertype=abstract)
755 [artid=18287&tool=pmcentrez&rendertype=abstract](http://www.pubmedcentral.nih.gov/articlerender.fcgi?artid=18287&tool=pmcentrez&rendertype=abstract)

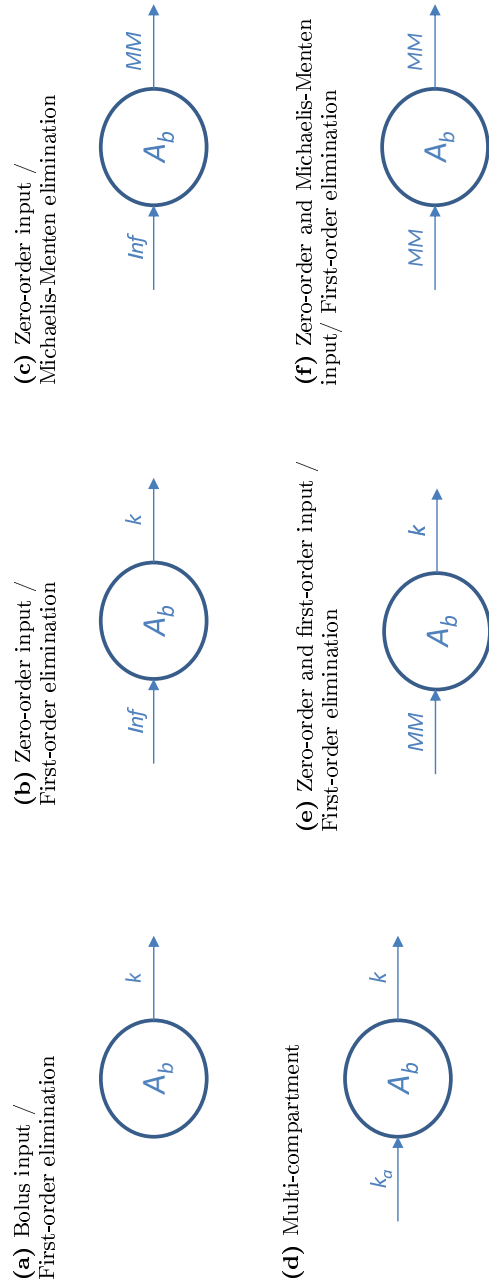

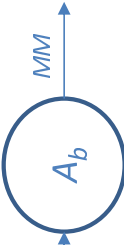




Figure 2: Examples drawn from a library biophase functions used here and in literature [21, 26, 64]. (a) bolus input and first-order elimination. (b) zero-order input and first-order elimination. (c) zero-order input and Michaelis-Menten elimination. (d) multi-compartment model. (e) zero-order and first-order input, and first-order elimination. (f) zero-order and Michaelis-Menten input, and first-order elimination. A_b , Inf , k , k_a , and MM represent, respectively, the biophase amount, the constant rate infusion input, the first-order elimination rate constant, the first-order absorption rate constant, and the Michaelis-Menten absorption/elimination process

Table 1: Evolution of the biophase model structure. Steps I - IV, description of the biophase function, the data used for the regression and the pair-wise accept/reject procedures when addressing the biophase disposition and absorption

Step	Model	Description	Data for regression
I		$\begin{cases} \text{Zero-order input} \\ \text{First-order elimination} \end{cases}$	Intravenous
II		$\begin{cases} \text{Zero-order input} \\ \text{Michaelis-Menten elimination} \end{cases}$	Intravenous
Pair-wise accept-reject procedure between the models in step I and step II. The zero-order input and first-order elimination model was considered the better model.			
III		$\begin{cases} \text{Zero-order input (IV}^a\text{)} \\ \text{First-order input (PO}^b\text{)} \\ \text{First-order elimination} \end{cases}$	Intravenous and oral
IV		$\begin{cases} \text{Zero-order input (IV}^a\text{)} \\ \text{Michaelis-Menten input (PO}^b\text{)} \\ \text{First-order elimination} \end{cases}$	Intravenous and oral
Pair-wise accept-reject procedure between the models in step III and step IV. The Michaelis-Menten input and first-order elimination model was considered the better model.			
^a Intravenous ^b Oral			

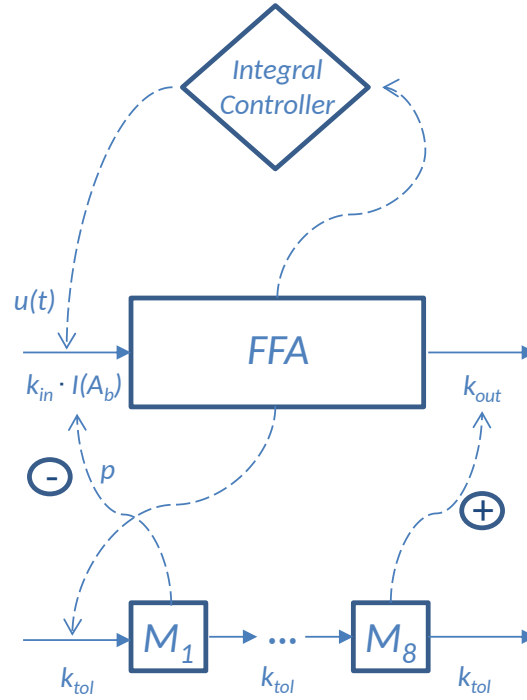


Figure 3: Schematic structure of the pharmacodynamics of the DRT feedback model. The pharmacodynamic model structure consists of a turnover equation coupled with a chain of moderator compartments, with slow and rapid feedback, as well as a slow integral control feedback. Here k_{in} denotes the turnover rate of FFA, k_{out} the fractional turnover rate of FFA, k_{tol} the turnover rate of the moderators, p the amplification factor, $I(A_b)$ the drug-mechanism function, and M_1 and M_8 the first and last moderator, respectively. Solid lines represent fluxes whilst the dashed lines represent flow of information (i.e., how the different entities affect one another)

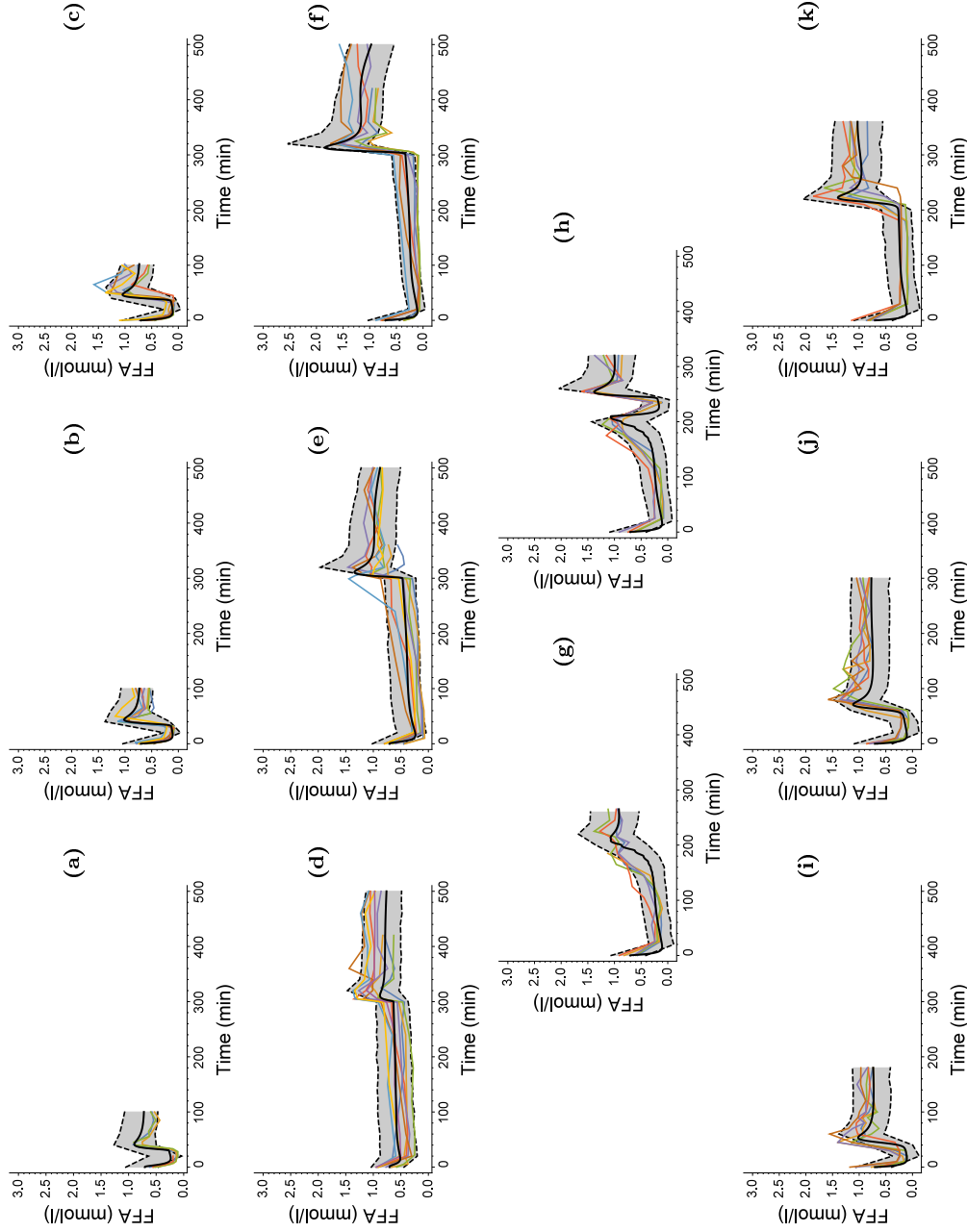


Figure 4: Population model fits to the FFA response levels, with 90% Monte Carlo prediction intervals. The black lines represent the estimated population median, the lower black dashed lines and the upper black dashed lines represent the 5%-quantile and the 95%-quantile of the Monte Carlo prediction interval, respectively. The coloured lines are the measured individual FFA response levels. (a-c) represent 30 min constant rate infusion of 0.017, 0.033, and 0.067 $\mu\text{mol kg}^{-1} \text{min}^{-1}$, respectively; (d-f) represent 300 min constant rate infusion of 0.17 $\mu\text{mol kg}^{-1} \text{min}^{-1}$ followed by a stepwise decrease in infusion rate to zero every 10 min for 180 min; (g) represents a 30 min constant rate infusion of 0.17 $\mu\text{mol kg}^{-1} \text{min}^{-1}$ followed by a stepwise decrease in infusion rate to zero every 10 min for 180 min; and (h) represents a 30 min constant rate infusion of 0.17 $\mu\text{mol kg}^{-1} \text{min}^{-1}$ followed by another 30 min constant rate infusion of 0.17 $\mu\text{mol kg}^{-1} \text{min}^{-1}$. (i-k) represent oral dosing of 24.4, 81.2, and 812 $\mu\text{mol kg}^{-1}$, respectively

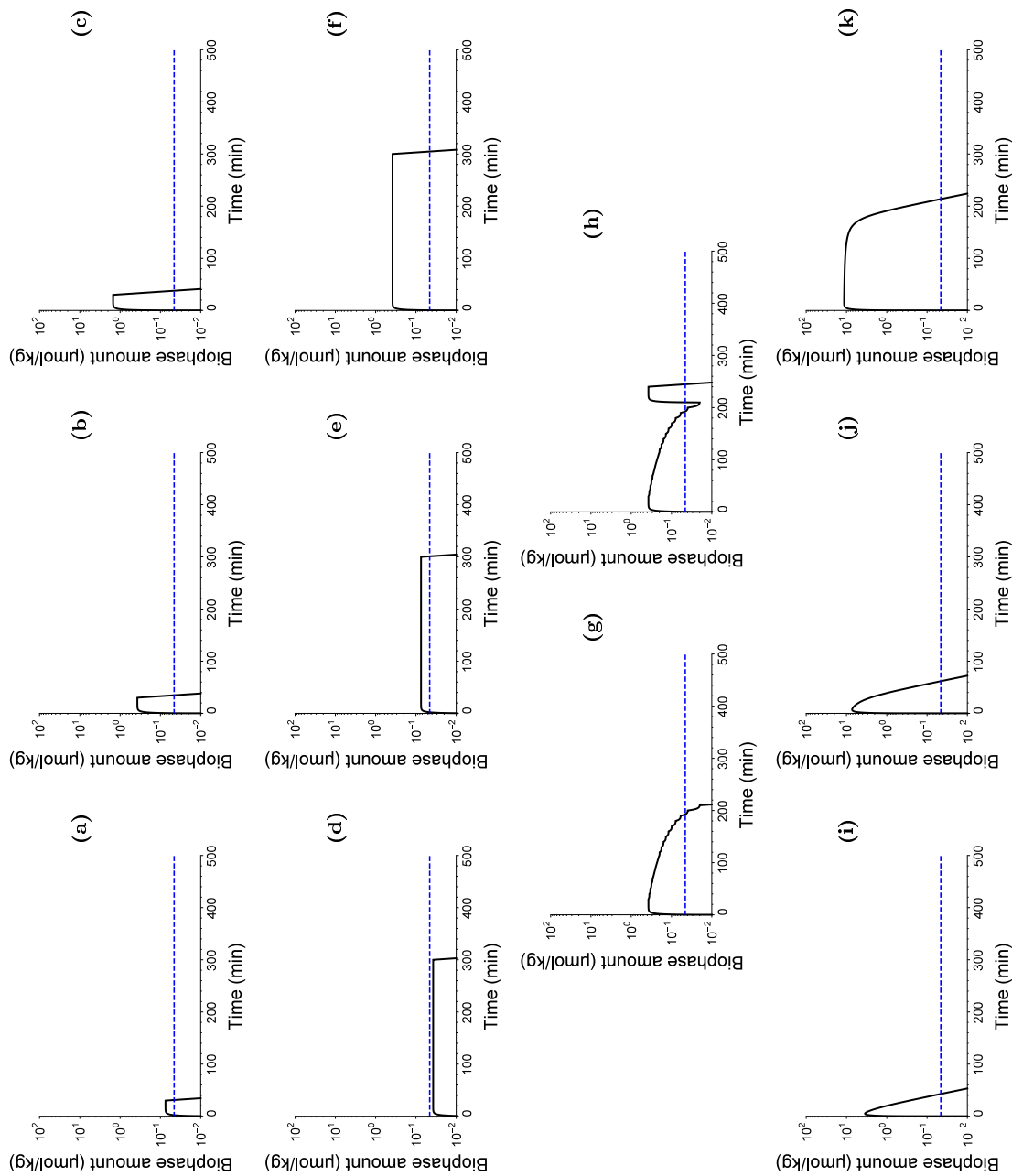


Figure 5: Population model predictions of the biophase drug amount on a semi-logarithmic scale. The black lines represent the estimated biophase drug amount and the blue dashed lines represent the predicted ID_{50} estimate. (a-c) represent 30 min constant rate infusion of 0.033, 0.17, and $0.67 \mu\text{mol kg}^{-1} \text{min}^{-1}$, respectively; (d-f) represent 300 min constant rate infusion of 0.017, 0.033, and $0.17 \mu\text{mol kg}^{-1} \text{min}^{-1}$, respectively; (g) represents a 30 min constant rate infusion of $0.17 \mu\text{mol kg}^{-1} \text{min}^{-1}$ followed by a stepwise decrease in infusion rate to zero every 10 min for 180 min; (h) represents a 30 min constant rate infusion of $0.17 \mu\text{mol kg}^{-1} \text{min}^{-1}$ followed by a stepwise decrease in infusion rate to zero every 10 min for 180 min and followed by another 30 min constant rate infusion of $0.17 \mu\text{mol kg}^{-1} \text{min}^{-1}$. (i-k) represent oral dosing of 24.4, 81.2, and $812 \mu\text{mol kg}^{-1}$, respectively

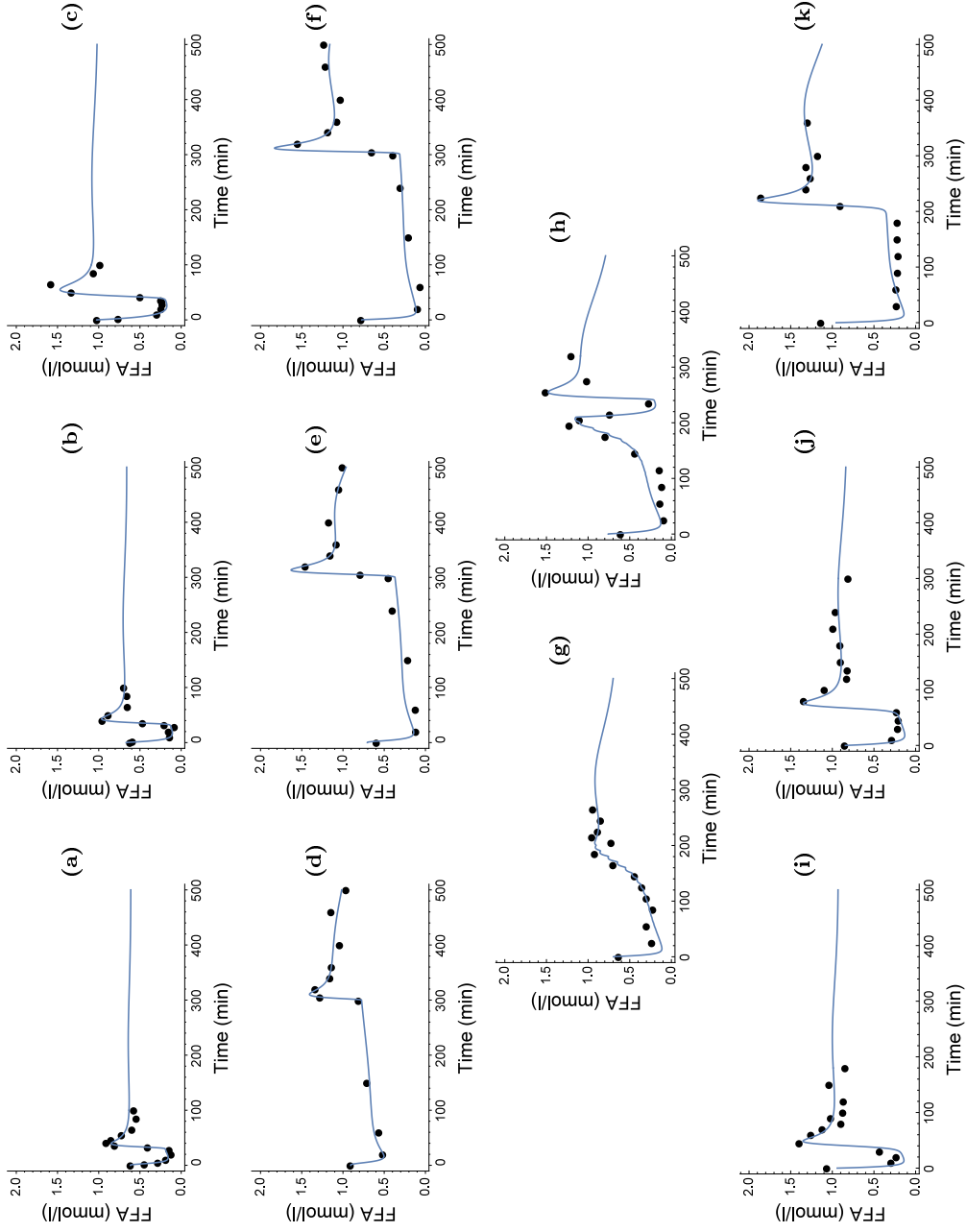


Figure 6: Individually fitted FFA response-time courses. (a-c) represent 30 min constant rate infusion of 0.033, 0.17, and 0.67 $\mu\text{mol kg}^{-1} \text{min}^{-1}$, respectively; (d-f) represent 30 min constant rate infusion of 0.017, 0.033, and 0.17 $\mu\text{mol kg}^{-1} \text{min}^{-1}$, respectively; (g) represents a 30 min constant rate infusion of 0.17 $\mu\text{mol kg}^{-1} \text{min}^{-1}$ followed by a stepwise decrease in infusion rate to zero every 10 min for 180 min; (h) represents a 30-min constant rate infusion of 0.17 $\mu\text{mol kg}^{-1} \text{min}^{-1}$ followed by a stepwise decrease in infusion rate to zero every 10 min for 180 min and followed by another 30 min constant rate infusion of 0.17 $\mu\text{mol kg}^{-1} \text{min}^{-1}$ and (i-k) represent oral dosing of 24.4, 81.2, and 812 $\mu\text{mol kg}^{-1}$, respectively

Table 2: DRT model parameter estimates and inter-individual variations, expressed in CV%, with corresponding relative standard errors (RSE%), and η -shrinkages

Parameter	Definition	Estimate	IV	η -shrinkage
$V_{\max,g}$ ($\mu\text{mol kg}^{-1} \text{min}^{-1}$)	Max. elimination rate from gut	5.37(0.97)	-	-
$K_{m,g}$ ($\mu\text{mol kg}^{-1}$)	Amount in gut at half $V_{\max,g}$	37.1(3.4)	-	-
k (min^{-1})	Biophase elimination rate	0.446(5.8)	45.1(23)	21%
R_0 (mmol l^{-1})	Baseline FFA conc.	0.705(2.3)	21.1(37)	4.2%
k_{out} (min^{-1})	Fractional turnover rate	0.306(8.1)	42.4(47)	46%
k_{tol} (min^{-1})	Turnover rate of moderator	0.0242(5.2)	24.4(98)	52%
K_1 (min^{-1})	Adaptation rate	0.00174(25)	90.6(23)	58%
p	Amplification factor	0.819(4.7)	-	-
I_{\max}	Efficacy	0.881(2.8)	-	-
ID_{50} ($\mu\text{mol kg}^{-1}$)	Potency	0.0456(6.8)	-	-
γ	Hill exponent	2.96(8.6)	-	-

Table 3: Estimated system rate constants and their corresponding half-lives (in minutes) with 90% non-parametric bootstrap prediction intervals

Parameter	Estimate	Half-life	90% PI ^a
k_{out} (min^{-1})	0.31	2.3	[1.3, 4.0]
k_{tol} (min^{-1})	0.024	29	[15, 51]
K_i (min^{-1})	0.0017	400	[210, 710]

^a90% non-parametric bootstrap prediction interval

Table 4: Comparison between the dynamic parameter estimates from the DRT study and an exposure-driven study. The parameter estimates are given with corresponding relative standard errors (RSE%)

Parameter	DRT analysis	Exposure-response anal.
k_{out} (min^{-1})	0.306(8.1)	0.244(7.3)
k_{tol} (min^{-1})	0.0242(5.2)	0.0222(2.7)
K_i (min^{-1})	0.00174(25)	0.00160(18)
p	0.819(4.7)	0.859(3.7)
I_{max}	0.881(2.8)	0.907(0.63)
γ	2.96(8.6)	2.36(9.2)

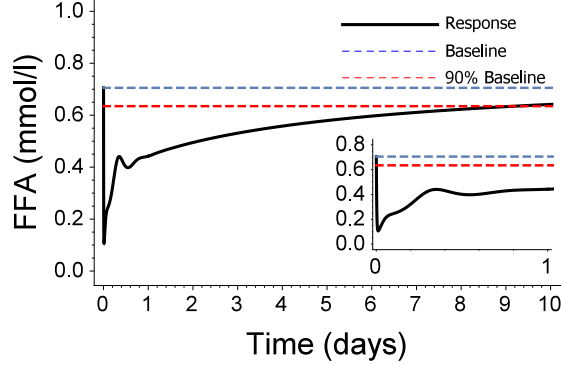


Figure 7: The long-term model-predicted effect of NiAc provocation on FFA level in normal rats with an infusion rate of $0.17 \mu\text{mol kg}^{-1} \text{min}^{-1}$ (aiming at a therapeutic NiAc concentration of $1 \mu\text{mol}$ [4]) during 10 days. The inserted figure shows in more detail the dynamics during the first day of NiAc infusion

Table 5: Model residual additive errors with corresponding relative standard errors (RSE%) and ε -shrinkage for infusion and oral data, respectively

Data	Residual add. error σ	ε -shrinkage
Infusion	0.0982(14)	9.5%
Oral	0.149(5.0)	7.7%

Specify fixed parameter rules and random effects (transform lmax to keep it bounded)

```
fixedParamRules = {kin → R0 * kout, lmax → 1 / (1 + Exp[-θ1])};
randomEffects = {kb → (kb * Exp[η1]), Ki → (Ki * Exp[η2]),
  R0 → (R0 * Exp[η3]), kout → (kout * Exp[η4]), ktol → (ktol * Exp[η5])};
```

Define system, initial conditions and measured variables

```
sys = {Ab'[t], R'[t], M1'[t], M2'[t],
  M3'[t], M4'[t], M5'[t], M6'[t], M7'[t], M8'[t], y'[t]} =
{bioInput - kb * Ab[t], (1 + Ki * y[t]) * kin *
  (1 - lmax * Ab[t]^γ / (ID50^γ + Ab[t]^γ)) * (R0 / M1[t])^p -
  kout * R[t] * (M8[t] / R0), ktol (R[t] - M1[t]),
  ktol (M1[t] - M2[t]), ktol (M2[t] - M3[t]),
  ktol (M3[t] - M4[t]), ktol (M4[t] - M5[t]),
  ktol (M5[t] - M6[t]), ktol (M6[t] - M7[t]),
  ktol (M7[t] - M8[t]), 1 - R[t] / R0};
ic = {Ab[0], R[0], M1[0], M2[0], M3[0], M4[0], M5[0], M6[0], M7[0], M8[0], y[0]} =
{0, R0, R0, R0, R0, R0, R0, R0, R0, R0, 0};
out =
{R[
  t]};
```

```
oralSys = {Aa'[t], Ab'[t], R'[t], M1'[t], M2'[t],
  M3'[t], M4'[t], M5'[t], M6'[t], M7'[t], M8'[t], y'[t]} =
{-aVmax * Aa[t] / (aKm + Aa[t]), bioInput - kb * Ab[t],
  (1 + Ki * y[t]) * kin *
  (1 - lmax * Ab[t]^γ / (ID50^γ + Ab[t]^γ)) * (R0 / M1[t])^p -
  kout * R[t] * (M8[t] / R0),
  ktol (R[t] - M1[t]), ktol (M1[t] - M2[t]), ktol (M2[t] - M3[t]),
  ktol (M3[t] - M4[t]), ktol (M4[t] - M5[t]), ktol (M5[t] - M6[t]),
  ktol (M6[t] - M7[t]), ktol (M7[t] - M8[t]),
  1 - R[t] / R0};
oralIc = {Aa[0], Ab[0], R[0], M1[0], M2[0], M3[0], M4[0], M5[0], M6[0], M7[0],
  M8[0], y[0]} = {absInput, 0, R0, R0, R0, R0, R0, R0, R0, R0, 0};
```

Specify input

```
bioInputFunctions = {RATE * UnitStep[DOSE / RATE - t], RATE * UnitStep[30 - t] +
  Piecewise[{{RATE - Ceiling[(t - 30) / 10] * RATE / 19, t > 30 && t < 210}}] +
  Piecewise[{{RATE * UnitStep[210 + (DOSE - 20) / RATE - t], t > 210}}],
  Aa[t] * aVmax / (aKm + Aa[t])};
absInputFunctions = {RATE * DOSE};
```

Specify systems

```
infSys = sys /. Thread[bioInput → bioInputFunctions[[1]]] /. fixedParamRules;
stepSys = sys /. Thread[bioInput → bioInputFunctions[[2]]] /. fixedParamRules;
oralSys = oralSys /. Thread[bioInput → bioInputFunctions[[3]]] /. fixedParamRules;
Define random variables (i.e. multiplicative random noises to certain parameters, here ID50, kout,
R0 and Ki)
```

```
randomParams = {η1, η2, η3, η4, η5};
Setting up models consisting of {sys}, {ic}, out
model1 = {{infSys}, {ic}, out} /. randomEffects;
model2 = {{stepSys}, {ic}, out} /. randomEffects;
model3 = {{oralSys}, {ic}, out} /. randomEffects;
{oralIc} /. Thread[absInput → absInputFunctions], out} /. randomEffects;
models = {model1, model2, model3};
Define Omega (interindividual variation)
L = {{ω11, 0, 0, 0, 0}, {0, ω22, 0, 0, 0},
  {0, 0, ω33, 0, 0}, {0, 0, 0, ω44, 0}, {0, 0, 0, 0, ω55}};
Ω = L.Transpose[L];
Define the S matrix for all models (measurement noise)
S1 = {{s1}};
S2 = {{s2}};
S3 = {{s3}};
sList = {s1, s2, s3};
Construct a data list of data from all models. In this case, with only one administration route, the list
only consains a single model.
```

```
infData = {Join[prepDataDose0Time0, prepDataDose1Time30,
  prepDataDose5Time30, prepDataDose20Time30, prepDataDose5Time300,
  prepDataDose10Time300, prepDataDose5Time300]};
stepData = {Join[prepDataDose20, prepDataDose25]};
oralData =
{Join[prepDataOralDose24, prepDataOralDose81, prepDataOralDose812]};
data = Join[infData, stepData, oralData];
Define all non yet defined constants of the system
listOfInputs = {DOSE, RATE};
Construct a parameter list with all the parameters
parameterStartValue = {{aVmax, 5}, {aKm, 30}, {θ1, 2}, {kb, 0.3}, {Ki, 0.001},
  {ID50, 0.05}, {kout, 0.30}, {R0, 0.70}, {γ, 1}, {ktol, 0.03}, {p, 1}};
ωStartValue = {{ω11, 0.1}, {ω22, 0.1}, {ω33, 0.1}, {ω44, 0.1}, {ω55, 0.1}};
sStartValue = {{s1, 0.1}, {s2, 0.1}, {s3, 0.1}};
fullParameterList = Join[params, {s1, s2, s3}];
Estimation of parameters
{pExpValues, pValues, history} =
FitPopulationModel[data, models, listOfInputs, parameterStartValue,
  {sList, sStartValue}, {randomParams, Ω, ωStartValue}, t, fullParameterList];
```